25th ABCM International Congress of Mechanical Engineering
October 20-25, 2019, Uberlândia, MG, Brazil

COB-2019-0703
USE OF MULTIPLE INERTIAL MEASUREMENT UNITS FOR INERTIAL NAVIGATION

Gilberto de Oliveira Costa
José Maurício S. T. Motta
Universidade de Brasília Departamento de Engenharia Mecânica Campus Darcy Ribeiro - Asa Norte Brasília - DF CEP: 70910-900
gilberto.costa@aluno.unb.br
jmmotta@unb.br

Abstract. *Mobile robots and other vehicles often can not have their movements fully described by the use of odometry, or other simpler ways of measuring the velocities of their actuators. For a good description of the movement of robots and other vehicles, it is possible to use inertial sensors, which allow the calculation of the position and orientation, without the dependence of signals appropriate to the calculation provided by the actuators. An approach to the use of multiple inertial sensors for the instantaneous center of rotation measurement can be used to describe the motion of vehicles where the non-slip feature can not be guaranteed. In order for low-cost accelerometers to be used for inertial navigation, they must be properly calibrated and their construction errors properly compensated. The task of identifying the correction parameters for the inertial measurement sensors can be performed using the Levenberg-Marquadt algorithm, a numerical algorithm for the solution of nonlinear equations.*
Keywords: *inertial navigation; inertial measurement units; sensor fusion; mobile robotics; skid-steering robots;*

1. INTRODUCTION

Mobile robot modeling with wheels has already been well described for most robots (Campion *et al.*, 1996), but for slip-steer robots, movement can not be described only by the use of odometry (Caracciolo *et al.*, 1999) (Kozłowski and Pazderski, 2004) (Kozłowski and Majchrzak, 2002) (Mafrica, 2012) (Pazderski *et al.*, 2004). Even with the use of advanced models based on vehicle dynamics (Kozłowski and Pazderski, 2004) (Yi *et al.*, 2009) the expected results for the use of odometry are often not satisfactory.

The use of inertial sensors can be a simple way to perform the calculation of the position of vehicles, even those that can be described more simply. Although the response of the reading of inertial sensors is an important tool for the estimation of vehicle position, the need to integrate these readings does not always produce good results and the result differs with each new integration required.

The calculation of the instantaneous center of rotation allows to describe with great quality the movement of mobile robots (and other vehicles), and since it doesn't require integration for the description of the movement, it is a good option for the use of low-cost inertial measurement units (IMU).

The objective of this work is to demonstrate the benefits of using multiple inertial measurement units to calculate the instantaneous center of rotation and thereby enable the use of low-cost inertial sensors to estimate the location of vehicles without bland holonomic constraints.

2. METHODOLOGY

Inertial navigation is a technique that uses an autonomous system to measure the movement of a vehicle and determine how far it has moved from its starting point. Acceleration is a vector quantity involving magnitude and direction. A single accelerometer measures magnitude but not direction. Typically, it measures the acceleration component along a predetermined line or direction. Steering information is usually provided by gyros that provide a frame of reference for accelerometers. Unlike other positional methods that depend on external references, an inertial navigation system is compact and autonomous, as it is not necessary to communicate with other stations or other references. This property allows the craft to navigate in an unknown territory (Webster, 1998).

Inertial navigation can be described as a process of directing the movement of a vehicle, rocket, ship, aircraft, robot, etc. from one point to another relative to a reference axis. The current position of the vehicle can be determined from the displacement relative to a known initial reference position (Webster, 1998). Controlling action is based on the sensor components of vehicle acceleration in known spatial directions, by instruments that mechanize the Newtonian laws of motion. The first and second integration of the detected acceleration determines velocity and position, respectively. For

the use of low-cost inertial sensors, sensor noise can cause many integration problems and should therefore be avoided.

For a better determination of the correction parameters of the readings of inertial measurement units, such as gain, constant level and crossed reading angles, using the Levenberg-Marquardt algorithm allows parameter values of the sensors are calculated so that the Euclidean norm of measurement errors can be minimized (Motta *et al.*, 2001) (Motta *et al.*, 2016).

Multiple IMUs can be used to: common mode noise correction between sensors; compensation of external forces not modeled; Gravitational force compensation; compensation of individual sensor rotation center readings very close to sensor positions; correction of incorrect readings of individual sensors.

The centrifugal acceleration can be represented by Eq. (1).

$$\vec{a_c} = \begin{bmatrix} \dot{\theta}_y^2 + \dot{\theta}_z^2 & -\dot{\theta}_x\dot{\theta}_y & -\dot{\theta}_x\dot{\theta}_z \\ -\dot{\theta}_x\dot{\theta}_y & \dot{\theta}_x^2 + \dot{\theta}_z^2 & -\dot{\theta}_y\dot{\theta}_z \\ -\dot{\theta}_x\dot{\theta}_z & -\dot{\theta}_y\dot{\theta}_z & \dot{\theta}_x^2 + \dot{\theta}_y^2 \end{bmatrix} . \begin{bmatrix} r_x \\ r_y \\ r_z \end{bmatrix} \tag{1}$$

The tangential acceleration can be expressed by Eq. (2).

$$\vec{a_t} = \begin{bmatrix} 0 & \ddot{\theta}_z & -\ddot{\theta}_y \\ -\ddot{\theta}_z & 0 & \ddot{\theta}_x \\ -\ddot{\theta}_y & \ddot{\theta}_x & 0 \end{bmatrix} . \begin{bmatrix} r_x \\ r_y \\ r_z \end{bmatrix} \tag{2}$$

The acceleration measured by the sensors can be obtained by the sum of Eq. (1) e da Eq. (2), resulting in Eq.(3).

$$\vec{a} = \vec{a_c} + \vec{a_t} = \begin{bmatrix} \dot{\theta}_y^2 + \dot{\theta}_z^2 & \ddot{\theta}_z - \dot{\theta}_x\dot{\theta}_y & -\ddot{\theta}_y - \dot{\theta}_x\dot{\theta}_z \\ -\ddot{\theta}_z - \dot{\theta}_x\dot{\theta}_y & \dot{\theta}_x^2 + \dot{\theta}_z^2 & \ddot{\theta}_x - \dot{\theta}_y\dot{\theta}_z \\ -\ddot{\theta}_y - \dot{\theta}_x\dot{\theta}_z & \ddot{\theta}_x - \dot{\theta}_y\dot{\theta}_z & \dot{\theta}_x^2 + \dot{\theta}_y^2 \end{bmatrix} . \begin{bmatrix} r_x \\ r_y \\ r_z \end{bmatrix} \tag{3}$$

By restricting the movement of the robot to the xy plane, the Eq. (3) may be expressed by Eq. (4).

$$\vec{a} = \begin{bmatrix} \dot{\theta}_z^2 & \ddot{\theta}_z & 0 \\ -\ddot{\theta}_z & \dot{\theta}_z^2 & 0 \\ 0 & 0 & 0 \end{bmatrix} . \begin{bmatrix} r_x \\ r_y \\ r_z \end{bmatrix} \tag{4}$$

For Eq. (4), the radius r_z can not be determined (even if by definition it is 0), so Eq. (4) can still be written in the form of Eq. (5).

$$\vec{a} = \begin{bmatrix} \dot{\theta}_z^2 & \ddot{\theta}_z \\ -\ddot{\theta}_z & \dot{\theta}_z^2 \end{bmatrix} . \begin{bmatrix} r_x \\ r_y \end{bmatrix} \tag{5}$$

Solving the system of Eq. (5), is defined as Eq. (6).

$$\begin{bmatrix} r_x \\ r_y \end{bmatrix} = \frac{1}{\dot{\theta}_z^4 + \ddot{\theta}_z^2} \begin{bmatrix} \dot{\theta}_z^2 & \ddot{\theta}_z \\ -\ddot{\theta}_z & \dot{\theta}_z^2 \end{bmatrix} . \begin{bmatrix} a_x \\ a_y \end{bmatrix} \tag{6}$$

The calculation of the instantaneous center of rotation allows the movement of the vehicle to be described with great precision and without the need for integration to be performed for its use. The Fig. 1a and Fig. 1b represent examples of readings of the resulting accelerations for a radius of rotation of 1m of the angular acceleration of $0.5rad/s^2$ and angular velocity of $0.5rad/s$,and of the angular acceleration of $-0.25rad/s^2$ and angular velocity of $-0.25rad/s$, respectively.

Figures 2a and 2b represent the readings of the expected measurements of the accelerations resulting from the angular acceleration of $-0.25rad/s^2$ and the angular velocity of $1rad/s$ and the angular acceleration of $-0.25rad/s^2$ and angular velocity of $0.5rad/s$, respectively.

2.1 Assembling description for the experiment

The experiment of measuring the instantaneous centers of rotation consists of using the accelerometers and gyrometers to calculate the positions r_x and r_y of the instantaneous centers of rotation with their measurements.

In order to carry out the measurements, a system was assembled whose block diagram can be seen in Fig. 3a.

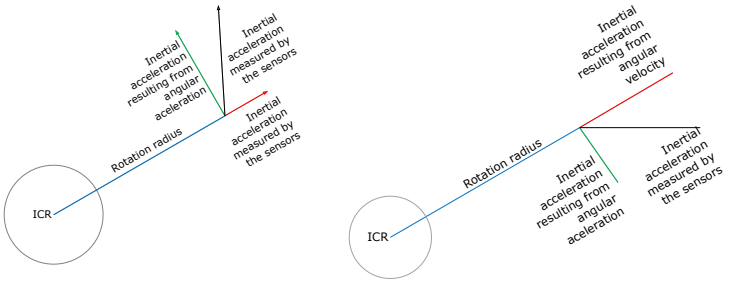

(a) (b)

Figure 1: Accelerations resulting from angular acceleration and angular velocity for a radius of 1m. (a) angular acceleration of $0.5rad/s^2$ and angular velocity of $0.5rad/s$, (b) angular acceleration of $-0.25rad/s^2$ and angular velocity of $0.71rad/s$

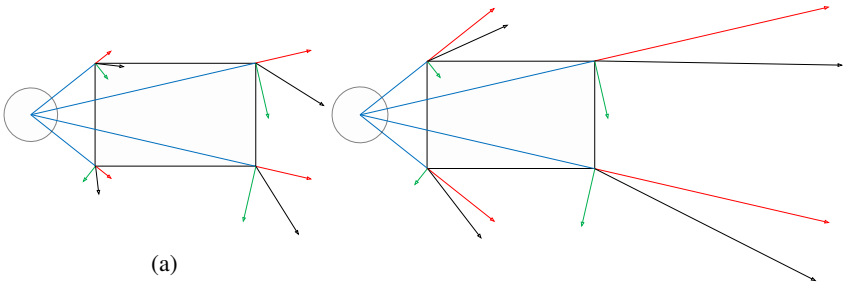

(a) (b)

Figure 2: Accelerations resulting from angular acceleration and angular velocity for 4 inertial measurement units, (a) angular acceleration of $-0.25rad/s^2$ and angular velocity of $1rad/s$, and (b) angular acceleration of $-0.25rad/s^2$ and angular velocity of $0.5rad/s$

Four MPU-6050s each containing the three accelerometers and three orthogonally mounted gyrometers in the IMU so that each is capable of measuring the respective linear accelerations and angular velocities of each of the three axes of the respective coordinate systems. The MPU-6050s are connected to the micro controller STM32F103 through a I^2C bus for values reading. The micro controller STM32F103 is responsible for calculating the position of the instantaneous centers of rotation of each set of the three accelerometers and three gyrometers, as well as the instantaneous center of rotation of the robot. The STM32F103 is connected to the ATmega328 micro controller through the I^2C bus. The ATmega328 micro controller is responsible for communication between the P-3AT robot, the STM32F103 micro controller and the computer that will collect the data and request multiple instant centers of rotation and angular velocities. For the communication between the robot P-3AT and the ATmega328 micro controller, a RS-232 serial communication port was used, which requires a voltage level shifter MAX-3232 for the connection between the robot and the micro controller. To simplify the connection and to enable communication between the ATmega328 micro controller and the computer, a pair of nRF24L01 radios connected through the micro controller SPI bus is used.

Figure 3b, shows the assembly sketch of the block elements of Fig. 3a. The MPU-6050 were equally spaced 96mm in the x direction of the robot's coordinate system in order to take advantage of the existing drilling, and equally spaced 150mm in the y direction, so that the sensors were within the protection of the top cover.

The MPU-6050 was mounted with its x measuring axis pointed out of the robot. This assembly has two main objectives: to facilitate the assembly of sensor cabling, and to try to reduce the common mode noise of the robot's acceleration reading. A photo of the robot assembly can be seen in Fig. 3c.

For the accomplishment of the tests for validation of the characteristics of the accelerometers and gyrometers, a very similar assembly was realized in the robot ABB IRB-140. This assembly can be visualized in Fig. 4a e 4b.

2.2 Modeling for parameters identification of accelerometers

Modeling for parameter identification can be performed by applying the Levenberg-Marquardt algorithm for the numerical solution to obtain the required parameters (Motta *et al.* (2001)).

In order to carry out the estimation of the values with fixed bias, scale factor, input axis misalignment and cross coupling of the input shaft, the accelerometers must be observed as a function that, from several geometric parameters of links and joint variables, is represented in Eq. (7). To identify only the nominal model, only non-zero values can be considered as parameters.

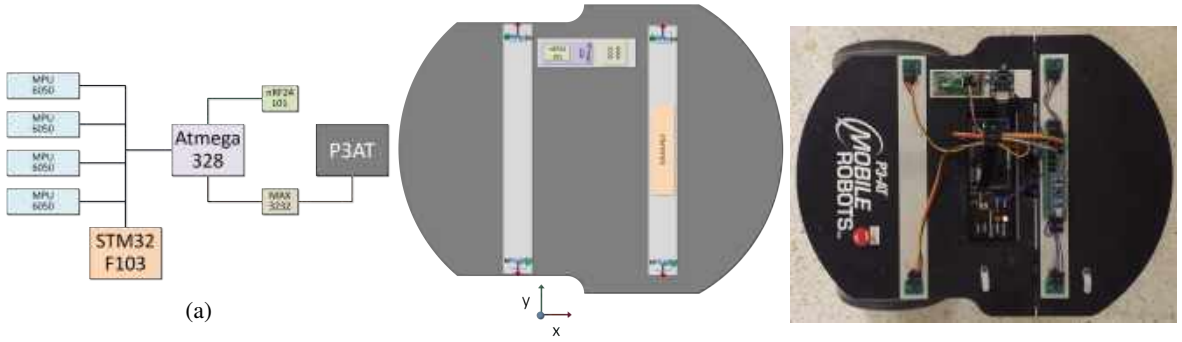

(a) (b) (c)

Figure 3: Figure 3a represents the block diagram of the sensor, (3b) the sketch and (3c) the sensor assembling on the P-3AT robot.

(a) (b)

Figure 4: Views of sensors mounted on IRB-140. (3b) shows the front view, and (3b) shows the view in the working orientation.

$$\vec{a} = f(\alpha, \beta, \gamma, o_x, o_y, o_z, g_x, g_y, g_z) \tag{7}$$

where: $\vec{a}$ represents the acceleration value measured by the sensor; α, β e γ are the pitch, roll and yaw angles of the sensor; o_x, o_y e o_z, are the fixed biases of each axis; g_x, g_y e g_z are the scale factors of each axis.

The first derivative of Eq. (7), indicated in Eq. (8), corresponds to the measurement error of the accelerometers.

$$\Delta\widehat{\vec{a}} = \frac{\partial\widehat{\vec{a}}}{\partial\alpha}.\Delta\alpha + \frac{\partial\widehat{\vec{a}}}{\partial\beta}.\Delta\beta + \frac{\partial\widehat{\vec{a}}}{\partial\gamma}.\Delta\gamma + \frac{\partial\widehat{\vec{a}}}{\partial o_x}.\Delta o_x + \frac{\partial\widehat{\vec{a}}}{\partial o_y}.\Delta o_y + \frac{\partial\widehat{\vec{a}}}{\partial o_z}.\Delta o_z + \frac{\partial\widehat{\vec{a}}}{\partial g_x}.\Delta g_x + \frac{\partial\widehat{\vec{a}}}{\partial g_y}.\Delta g_y + \frac{\partial\widehat{\vec{a}}}{\partial g_z}.\Delta g_z \tag{8}$$

The value of $\widehat{\vec{a}}$ in Eq. (8) expresses the measurement error of the acceleration value measured by the accelerometers.

$$\Delta\widehat{\vec{a}} = M - C \tag{9}$$

where: M is the value measured by the sensors and C is the value calculated by the model.

Equation (8) can be rewritten in the matrix form, as expressed in Eq. (10). Thus, Eq. (9) is now formulated as the Jacobian matrix of the manipulator, consisting of the partial derivatives of $\vec{a}$ with respect to each parameter to be identified. The term Δx, present in Eq. (10), corresponds to the vector with the calibrated parameters. Therefore, the calibration problem is the solution of a system of nonlinear equations of the type **Ax = b**.

$$\Delta\widehat{\vec{a}} = \begin{bmatrix} \frac{\partial\widehat{\vec{a}}}{\partial\alpha}_1 & \frac{\partial\widehat{\vec{a}}}{\partial\beta}_1 & \cdots & \frac{\partial\widehat{\vec{a}}}{\partial g_z}_1 \\ \frac{\partial\widehat{\vec{a}}}{\partial\alpha}_2 & \frac{\partial\widehat{\vec{a}}}{\partial\beta}_2 & \cdots & \frac{\partial\widehat{\vec{a}}}{\partial g_z}_2 \\ \vdots & \vdots & \ddots & \vdots \\ \frac{\partial\widehat{\vec{a}}}{\partial\alpha}_m & \frac{\partial\widehat{\vec{a}}}{\partial\beta}_m & \cdots & \frac{\partial\widehat{\vec{a}}}{\partial g_z}_m \end{bmatrix} \cdot \begin{bmatrix} \Delta\alpha \\ \Delta\beta \\ \vdots \\ \Delta g_z \end{bmatrix} = J.\Delta x \tag{10}$$

Several methods are available to solve the system described in Eq. (10), among which the algorithm proposed by Levenberg-Marquardt, according to Dennis Jr and Schnabel (1996), which proved to be successful in practical terms, and is therefore recommended for general solutions. This is an iterative solution method, which introduces some changes in the Gauss-Newton method, in order to avoid problems related to numerical divergence.

The method implemented to identify the parameters of the accelerometers (Levenberg-Marquadt algorithm) can be found with details in the paper of Motta *et al.* (2016). Equation (11) can be used to represent the ideal model of acceleration reading by accelerometers.

$$\vec{a} = Rot(\alpha,\beta,\gamma)\vec{g} = \begin{bmatrix} C_\beta C_\gamma & C_\gamma S_\alpha S_\beta - C_\alpha S_\gamma & S_\alpha S_\gamma + C_\alpha S_\beta C_\gamma \\ C_\beta S_\gamma & C_\alpha C_\gamma + S_\alpha S_\beta S_\gamma & C_\alpha S_\beta S_\gamma - C_\gamma S_\alpha \\ -S_\beta & C_\beta S_\alpha & C_\alpha C_\beta \end{bmatrix} \begin{bmatrix} 0 \\ 0 \\ g \end{bmatrix} = \begin{bmatrix} S_\alpha S_\gamma + C_\alpha S_\beta C_\gamma \\ C_\alpha S_\beta S_\gamma - S_\alpha C_\gamma \\ C_\alpha C_\beta \end{bmatrix} g \quad (11)$$

where C_α, S_α, C_β, S_β, C_γ e S_γ, respectively $cos\alpha$, $sen\alpha$, $cos\beta$, $sen\beta$, $cos\gamma$ e $sen\gamma$.

The model for obtaining the correction parameters for the measurement errors of the accelerometers used is presented in Eq. (12).

$$\vec{a} = \begin{bmatrix} o_x + g_x(S_{\alpha\delta_\alpha} S_{\gamma\delta_\gamma} + C_{\alpha\delta_\alpha} S_{\beta\delta_\beta} C_{\gamma\delta_\gamma}) \\ o_y + g_y(C_{\alpha\delta_\alpha} S_{\beta\delta_\beta} S_{\gamma\delta_\gamma} - S_{\alpha\delta_\alpha} C_{\gamma\delta_\gamma}) \\ o_z + g_z(C_{\alpha\delta_\alpha} C_{\beta\delta_\beta}) \end{bmatrix} \quad (12)$$

where $C_{\alpha\delta_\alpha}$, $S_{\alpha\delta_\alpha}$, $C_{\beta\delta_\beta}$, $S_{\beta\delta_\beta}$, $C_{\gamma\delta_\gamma}$ e $S_{\gamma\delta_\gamma}$, respectively $cos(\alpha+\delta_\alpha)$, $sen(\alpha+\delta_\alpha)$, $cos(\beta+\delta_\beta)$, $sen(\beta+\delta_\beta)$, $cos(\gamma+\delta_\gamma)$ e $sen(\gamma+\delta_\gamma)$.

2.3 Proof of the measurement model of the instantaneous centers of rotation

To confirm the model of measurement of instantaneous centers of rotation three fundamental items are necessary:

1. The motion is performed exclusively on a plane, preferably horizontal, so that external forces, including the gravitational force, influence the experiment very little or none.
2. A distance to the center of rotation that is reliable and precisely measured, so that adjustments to the model are not necessary to prove its quality.
3. A known angular velocity, a known angular acceleration such that both can be properly modeled.

To meet the needs of the experiment, it was necessary to use the robot ABB IRB-140, which is a robot of six degrees of freedom whose base was mounted on a surface parallel to the horizontal plane, attending the first item necessary to carry out for an experiment appropriate.

The ABB IRB-140 robot is a robot with precise angular position, speed and acceleration satisfying the second and third items for the experiment.

The calculation of the angles and the distance of the robot end-effector relative to the center of rotation of its base was performed based on the direct and inverse kinematics of the ABB IRB-140 robot. As the movement towards the z-axis was not necessary to perform the experiment and did not influence its result, the calculations were simplified so that the robot behaved in a very similar way to a SCARA robot, where the planar movement is performed, for the most part, with the variation of only the joint axis 1.

Axes 2 and 3 are responsible for the constant radius of the circle of rotation (a great advantage of this experiment) and the axis 5 is used to ensure that the orientation of the sensors is kept horizontal. Axes 4 and 6 are set at zero degrees so that there is no variation of the angles α and β of the sensors.

3. RESULTS AND DISCUSSION

3.1 Parameters identification of the accelerometers

In order to validate the mathematical model proposed in Eq. (12), the accelerometers were submitted to several angles with which a set of data was supposed to be formed with which numerical methods, with the algorithm of Levenberg-Marquardt, were able to find the adjustments that would minimize the measurement errors.

For the experiment, the angles α (around the sensor's x-axis) were varied between $-90°$ and $90°$ with steps of $30°$ and β (about the y-axis of the sensor) were varied between $-180°$ and $180°$ with variation of $-30°$ for each of the sets of measurements, a total of 67 sets of measurements. For both values of α and β equal to 0, the z-axis of the sensor is perfectly perpendicular to the ground plane, ie the sensor reading should be equal to the acceleration of gravity.

Figure 5 illustrates the ABB IRB-140 robot in its home position pose, with a slight difference, the pulse was rotated upward twisting θ_5 to $90°$. The twisting θ_5 to $90°$ in this orientation makes the values of α and β of the accelerometer calibration model to be zero. To change these angles, the robot was required to move joint $theta_5$ in order to vary the angle $alpha$ and so joint θ_6 in order to vary the angle β. The value of α equals $\theta_5 - 90°$ and so value of β is equal to the value of θ_6.

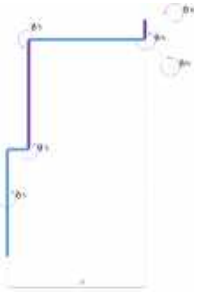

Figure 5: Home position pose of ABB IRB-140 with the wrist facing upwards

Figure 6a illustrates the response of the mathematical model proposed in Eq. (12) in reading the accelerometer measurement for the set of angles for which the experiment was proposed. In Fig. 6a it can be seen that the three axes of the accelerometers can be subjected to values of accelerations that vary with the range of positive and negative values of the acceleration of gravity.

The maximum value measured by each of the accelerometers should be 16384 units, which represents the acceleration of gravity at sea level, approximately $9.80665m/s^2$, when the sensor was precisely perpendicular to the plane of the ground.

The result obtained for the measurement of each of the four IMUs used in the experiment is observed in Fig. 6b.

After the application of the Levenberg-Marquardt algorithm, the parameters of Table 1 required for the correction of the reading were obtained, where o_k are the fixed bias of the accelerometers, g_k are the gains necessary for the measurement of the gravity, and δ_k are the angles (measured in degrees) of misalignments of the accelerometer axes.

Table 1: Required parameters for the calibration. The δ_k are expressed in degrees (°), and the o_k e g_k are expressed in the accelerometer units ($\approx 599\mu m/s^2$).

Parâmetro	o_x	o_y	o_z	g_x	g_y	g_z	δ_α	δ_β	δ_γ
IMU_1	216	-165	278	16466	16277	16439	0,398	0,113	0,314
IMU_2	-95	292	221	16480	16383	16775	0,374	0,204	-0,458
IMU_3	159	-135	7	16304	16309	16509	0,385	0,207	0,026
IMU_4	-596	99	-338	16341	16370	16524	0,354	0,235	0,110

After adjusting the values, the measurements are presented in Fig. 6c.

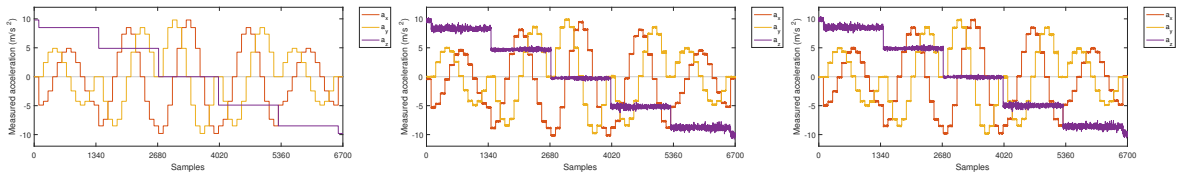

(a) (b) (c)

Figure 6: Acceleration measured by accelerometers. (a) shows the prediction performed by the application of Eq. 12, (b) shows the measurement of IMU_4 without parameters correction, and (c) shows the measurement of IMU_4 after parameters correction. Where a_x, a_y and a_z are the accelerations measureds on the x, y and z axis respectively.

The accelerometers behaved linearly even at values close to zero, so both the dead zone and the threshold are not present on this sensor or are smaller than the sensor resolution, however, for the readings of the accelerometer values have better noise rejections, a dead zone of 16 units has been added for all accelerometers ($\approx 10mm/s^2$).

3.2 Parameters Identification of the gyrometers

Although the procedure for obtaining the parameter values for the gyrometers was simpler, it was necessary to perform some steps to correct the measurement values. In order to measure the fixed bias of the gyrometers, they were subjected to a zero angular velocity ($\vec{\omega} = 0$). From the mean values of the measurements, the value of the fixed bias of the gyros is determined every time the IMUs are initialized.

The scale factor is determined from measured values of known angular velocities at which the gyrometers are subjected.

During the experiments, the gyrometers were subjected to the same set of angular velocities, and the values were compared for the validation of the predicted scale factor in the datasheet of the device.

As the accelerometers and the gyrometers were built on the same chip, it was assumed that the misalignment of the accelerometers and gyrometers mounting is the same.

The gyrometers behaved linearly at values very close to zero, so both the dead zone and the threshold are not present in this sensor or are smaller than the sensor resolution, however, for the readings of the gyrometer values have better noise rejections, a dead zone of 16 units has been added for all the gyrometers ($\approx 0.8 mrad/s$).

3.3 Measuring the instantaneous centers of rotation

The experiment was performed for several speeds and horizontal reaches for the validation of the proposed model to calculate the position of the sensors given by Eq. (6).

Based on Fig. 5 and the inverse kinematics of the IRB-140 robot, it is possible to calculate the horizontal distance from the end-effector element (where the sensor is located) to the base (instantaneous center of rotation). Since it is not necessary to calculate the height of the sensor to perform the experiment, the inverse kinematics can be simplified for Eq. (13).

$$\theta_2 = sin^{-1}\left(\frac{r - d_1 - l_3 * cos(\theta_{23})}{l_2}\right) \tag{13}$$

In Eq. (13), r is the radius, q_2 is the angle of joint 2, d_1 is the length of link 1, l_2 is the length of the link 2, l_3 is the length of link 3 and q_{23} is the sum of the angles of joints q_2 and q_3 (which for the experiment must equal zero). The radius r becomes negative when the end-effector is on the back of the manipulator.

The measurement of the angles and angular velocities can be performed according to Fig. 7. In Fig. 7, the radii are the distance from the center of mass (CoM) to the instantaneous center of rotation (ICR) measured in the axis Y_{CoM}. The angular velocity ω can be defined as the angular variation around the ICR. If the ICR is in a negative position of the axis Y_{CoM} the radius value r should be negative.

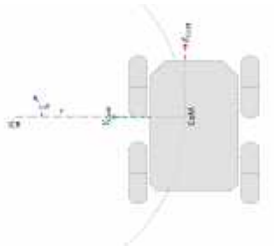

Figure 7: Definition of radius and angular velocity measurement

The results obtained are presented in Fig. 8 and Fig. 9.

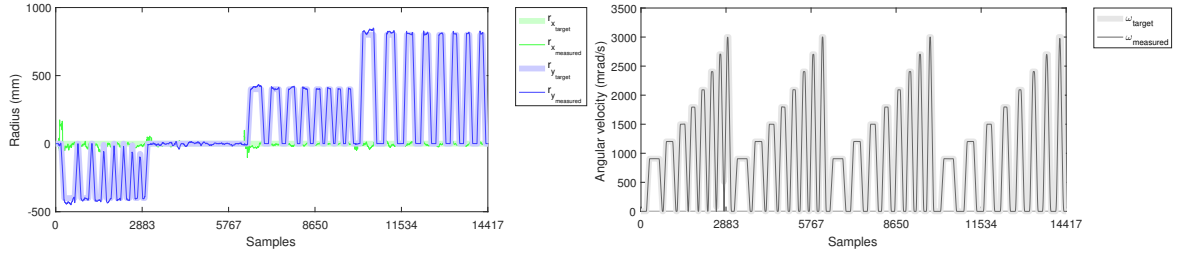

(a) (b)

Figure 8: Radius measurement between -400mm and 800mm, for angular velocities between 800mrad/s e 2800mrad/s. (a) shows measured radii and (b) shows messured angular velocities

As shown in Fig. 8, it can be verified that the angular velocity measurement by the gyroscope has a good response for angular velocities between 800mrad/s and 2800mrad/s and that it is also possible to measure radii for these velocities with a relatively good quality and that it can be tested on the Pioneer P-3AT mobile robot with great effectiveness. As shown in Fig. 9, the radius measurement for low angular velocities (between -700mrad/s and 700mrad/s) does not present a suitable quality of the radii measurements, although angular velocity measurements by gyroscope are good.

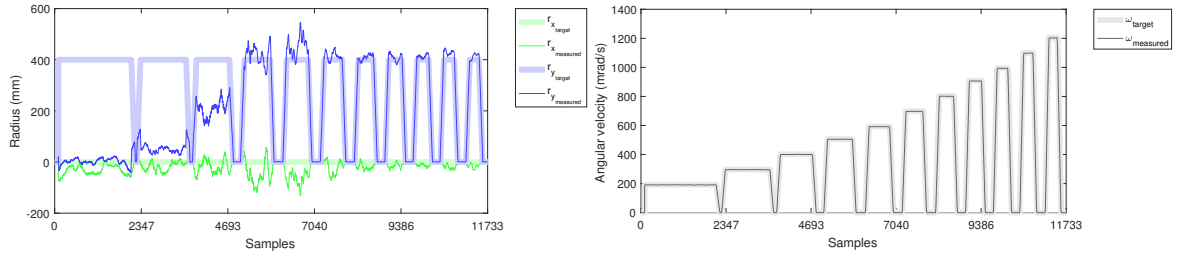

(a) (b)

Figure 9: Measurement of 400mm radius, for angular velocities between 200mrad/s e 1200mrad/s. (a) shows the measured radii and (b) shows the angular velocities.

4. CONCLUSIONS

The calibration of the accelerometers by the Levenberg-Marquardt method allowed low-cost accelerometers to have their construction parameters corrected and allowed these devices to be used to determine the instantaneous centers of rotation. For a robot in which other forms of positioning computation would be very complex, such as computer vision methods or other external measurement methods, position estimation using IMUs may be the best solution.

The calculation of the instantaneous rotation centers, because it is a low complexity computational operation, can be executed in real time even for micro controllers with low processing capacity, which makes its use ideal for use in embedded applications where, both the energy consumption and the processing capacity are crucial to a good result.

For the experiments carried out, it was verified that the mean error of the measurement of the values is less than 6 mm, or comparatively, 2% of the ICR calculated value, which makes it possible to use them for navigation applications. The use of multiple inertial measurement units to improve the quality of inertial navigation may be the ideal way to use low-cost sensors with high performance. Despite the increased computational cost, the many advantages of using multiple inertial measurement units make their use necessary when it is not possible to use sensors with better individual performance.

5. REFERENCES

Campion, G., Bastin, G. and Dandrea-Novel, B., 1996. "Structural properties and classification of kinematic and dynamic models of wheeled mobile robots". *IEEE transactions on robotics and automation*, Vol. 12, No. 1, pp. 47–62.

Caracciolo, L., De Luca, A. and Iannitti, S., 1999. "Trajectory tracking control of a four-wheel differentially driven mobile robot". In *Robotics and Automation, 1999. Proceedings. 1999 IEEE International Conference on*. IEEE, Vol. 4, pp. 2632–2638.

Dennis Jr, J.E. and Schnabel, R.B., 1996. *Numerical methods for unconstrained optimization and nonlinear equations*, Vol. 16. Siam.

Kozłowski, K. and Majchrzak, J., 2002. "A new control algorithm for a nonholonomic mobile robot". *Archives of Control Sciences*, Vol. 12, No. 1/2, pp. 37–69.

Kozłowski, K. and Pazderski, D., 2004. "Global positioning systems, inertial navigation, and integration". *International journal of applied mathematics and computer science*, Vol. 14, pp. 477–496.

Mafrica, S., 2012. "Advance modeling of a skid-steering mobile robot for remote telepresence". *Master theses*.

Motta, J.M.S., de Carvalho, G.C. and McMaster, R., 2001. "Robot calibration using a 3d vision-based measurement system with a single camera". *Robotics and Computer-Integrated Manufacturing*, Vol. 17, No. 6, pp. 487–497.

Motta, J.M.S., Llanos-Quintero, C.H. and Coral Sampaio, R., 2016. "Inverse kinematics and model calibration optimization of a five-dof robot for repairing the surface profiles of hydraulic turbine blades". *International Journal of Advanced Robotic Systems*, Vol. 13, No. 3, p. 114.

Pazderski, D., Kozłowski, K. and Dixon, W., 2004. "Tracking and regulation control of a skid steering vehicle". In *American Nuclear Society Tenth International Topical Meeting on Robotics and Remote Systems*. Gainesville, Florida, pp. 369–376.

Webster, J.G., 1998. *The measurement, instrumentation and sensors handbook*. CRC press.

Yi, J., Wang, H., Zhang, J., Song, D., Jayasuriya, S. and Liu, J., 2009. "Kinematic modeling and analysis of skid-steered mobile robots with applications to low-cost inertial-measurement-unit-based motion estimation". *IEEE transactions on robotics*, Vol. 25, No. 5, pp. 1087–1097.

6. RESPONSIBILITY NOTICE

The authors are the only responsible for the printed material included in this paper.